Overscreened Kondo fixed point in $S = 1$ spin liquid

Maksym Serbyn, T. Senthil, and Patrick A. Lee
Department of Physics, Massachusetts Institute of Technology, Cambridge, Massachusetts 02139, USA
(Received 8 March 2013; published 19 July 2013)

We propose a possible realization of the overscreened Kondo impurity problem by a magnetic $s = 1/2$ impurity embedded in a two-dimensional $S = 1$ $U(1)$ spin liquid with a Fermi surface. This problem contains an interesting interplay between non-Fermi-liquid behavior induced by a $U(1)$ gauge field coupled to fermions and a non-Fermi-liquid fixed point in the overscreened Kondo problem. Using a large-N expansion together with an expansion in the dynamical exponent of the gauge field, we find that the coupling to the gauge field leads to weak but observable changes in the physical properties of the system at the overscreened Kondo fixed point. We discuss the extrapolation of this result to a physical case and argue that the realization of overscreened Kondo physics could lead to observations of effects due to gauge fields.

DOI: 10.1103/PhysRevB.88.024419 PACS number(s): 71.27.+a, 71.10.Hf, 75.10.Kt, 72.10.Fk

I. INTRODUCTION

Impurity models constitute an important chapter in modern condensed-matter physics. Since the original paper by Kondo[1] considering an electron sea screening a single-impurity spin, this problem has attracted significant theoretical and experimental attention.[2–20] More recently, impurity physics has been studied in the context of strongly interacting systems. Numerous examples include[21] an impurity in systems with vanishing density of states,[22,23] high-temperature superconductors,[24] and quantum magnets.[25–30] Quantum magnets are particularly versatile as a host system, having a large number of possible ground states with different low-energy excitations.

In this paper we consider a spin-half impurity embedded in a spin-1 quantum paramagnet with a spin-liquid ground state.[31] We consider the situation where the low-energy excitations of the paramagnet are described by emergent fermionic excitations with a Fermi surface, coupled to a $U(1)$ gauge field. This study is motivated by the recent appearance of several $S = 1$ spin-liquid candidate materials.[32,33] Theoretically, a number of spin-liquid ground states for a spin-1 system have been proposed.[34–41] One possible scenario involves the emergence of three fermionic excitations carrying spin-1 quantum numbers.[37,39,41] Assuming that Fermi surfaces of these excitations are not destroyed by a pairing instability, we obtain the host system that is considered below.

Impurity physics in a spin-1/2 spin liquid has been considered in the context of bosonic spin liquids,[26] algebraic spin liquids,[27,28] and spin liquids with a Fermi surface.[30] In particular, Ribeiro and Lee[30] concluded that the physics of a spin-1/2 impurity embedded in a spin liquid with $S = 1/2$ fermionic excitations is similar to that of the conventional Kondo problem.[14] In what follows we argue that a spin-1/2 impurity in a $S = 1$ spin liquid with a Fermi surface realizes overscreened Kondo physics. Although our results are qualitatively similar to the overscreened Kondo effect in conventional systems, there are observable differences due to the presence of an emergent gauge field coupled to spinons.

Our findings suggest that an impurity in a $S = 1$ spin liquid can be used to probe fermionic excitations. As these excitations do not carry a charge, their experimental detection is a difficult problem. Different experimental probes have been suggested in the context of spin-1/2 spin liquids.[42–47] We suggest that the realization of overscreened Kondo physics is a possible way to unravel the physics of a spin-1 spin liquid, allowing probes of fermionic excitations, as well as the presence of an emergent gauge field.

Overscreened Kondo physics is realized in multichannel Kondo models, where a single spin is coupled to N copies (flavors) of itinerant electrons.[4] On the one hand, such a generalization of the original Kondo model may be seen as merely a theoretical tool, allowing a perturbative expansion in $1/N$. On the other hand, the physics changes drastically depending on the interrelation between impurity spin length s and the number of flavors coupled to the impurity. When the number of flavors N is just enough or less than needed to screen the impurity spin, $N \leqslant 2s$, antiferromagnetic coupling between the impurity and electrons flows to infinity in the infrared, meaning that at low temperatures impurity spin is screened to the maximum possible extent by electrons. For the case of perfect screening, $N = 2s$, this results in Fermi-liquid behavior.[5,14] In the underscreened case residual ferromagnetic interaction leads to a singular Fermi liquid.[48,49] However, in the overscreened regime, $N > 2s$, i.e., when there are more channels than required to screen the impurity spin, the system has a non-Fermi-liquid fixed point. [6,7,9,11] This state is characterized by singularities in different physical observables, such as impurity spin susceptibility, specific heat, etc. It is particularly interesting as a solvable example of a system with a non-Fermi-liquid fixed point.[6] Despite the rich and interesting physics, the overscreened regime of the Kondo model has only a few realizations (in particular quantum dots and two-level systems.[13,15,16,50]). Hence our system is also interesting as a possible implementation of overscreened Kondo physics.

Qualitatively, the problem of a spin-1/2 impurity hosted by an isotropic $S = 1$ spin liquid looks similar to the conventional overscreened Kondo impurity model. When coupled antiferromagnetically, itinerant excitations carrying spin-1 quantum numbers cannot screen the impurity. However, the presence of a gauge field effectively enforcing a single-occupancy constraint for fermionic excitations makes these two problems different. Even without the impurity, fermions are in a non-Fermi-liquid regime[51–57] due to the gauge field. The fermion propagator is dressed by a singular self-energy, so there are no well-defined quasiparticle excitations in the system. This is

manifested, for example, in the singular behavior of the specific heat $C \propto T^{2/3}$ in two dimensions at low temperatures.[51,55]

Coupling the impurity to fermions with non-Fermi-liquid behavior allows us to study the interplay between the gauge field induced non-Fermi-liquid behavior and the Kondo non-Fermi-liquid fixed point. The conventional approach to the Kondo problem is either an exact solution by mapping it onto a one-dimensional problem[6,19] or $1/N$ expansion. Neither method is directly applicable in our case. The presence of a gauge field impedes the mapping of our model to a one-dimensional problem in the radial channel. On the other hand, a rigorous $1/N$ expansion is not possible due to singular self-energy corrections.[56,58] The latter issue has been recently resolved in the paper by Mross *et al.*,[57] where a controlled double-expansion scheme has been provided. It combines the $1/N$ expansion with an expansion in another small parameter (related to the dynamical critical exponent of the gauge field).

We adapt the recently developed double-expansion method[57] to our problem. Since the double expansion includes the large N limit, we expect to have a perturbatively accessible fixed point. At leading order, the gauge field does not affect the position of this non-Fermi-liquid Kondo fixed point. However, it leads to corrections to the scaling dimension of the Kondo coupling. Assuming that the results obtained using the double expansion interpolate to the physical case, we conclude that physical properties such as impurity spin susceptibility, specific heat, etc., are still characterized by singular behavior. Unlike the case of the Kondo model in the regime of perfect screening,[30] where the coupling to the gauge field has no consequences to leading order in $1/N$, in our case the gauge field influences Kondo physics.

The rest of the paper is organized as follows. In the remainder of this section, we introduce the basics of our model and diagram technique and briefly explain the idea behind double expansion. In Sec. II we first review known results for the β function in the overscreened Kondo problem without the gauge field. Afterwards, we calculate the β function with the gauge field and study the changes in scaling behavior of different physical quantities. Finally, in Sec. III we discuss the extrapolation of our findings beyond the double expansion and comment on possible experimental realizations and experiments to detect Kondo physics. Details regarding the calculation of corrections to the β function due to the gauge field are given in Appendixes A and B.

A. Spin liquid with fermionic excitations and impurity

Let us consider a spin Hamiltonian on a lattice consisting of spin-1 sites,

$$H_{\text{spin}} = \sum_{ij} [J_{ij} \boldsymbol{S}_i \cdot \boldsymbol{S}_j + K_{ij} (\boldsymbol{S}_i \cdot \boldsymbol{S}_j)^2] + \cdots, \tag{1}$$

where the ellipsis denotes other possible terms such as ring exchange. We are motivated by recent work[41] which shows evidence of stabilizing a spin-liquid phase with spinon Fermi surface on a triangular lattice with nearest-neighbor bilinear and biquadratic spin interactions along with ring-exchange terms. The low-energy description of such a state is a theory of fermions strongly coupled to a $U(1)$ gauge field. From now on we assume that such a spin-liquid state exists and work only with the low-energy effective theory described below.

Referring the reader to the literature for more detailed discussions of the effective theory,[59] we only summarize the results. A spin-1 operator at a given site is represented using three fermion operators $\tilde{f}_\lambda$, $\lambda = 1,2,3$, as

$$\boldsymbol{S}_i = \sum_{\lambda,\rho=1}^{3} \tilde{f}^\dagger_{i\lambda} \boldsymbol{I}^{\lambda\rho} \tilde{f}_{i\rho}, \tag{2}$$

with $\boldsymbol{I}^{\lambda\rho}$ being the set of three spin-1 matrices [generators of $SU(2)$ in spin-1 representation].[37] In order to remove unphysical states from the Hilbert space, introduced by the representation in Eq. (2), one has to enforce a single-occupancy constraint on each site. Fermionic $\tilde{f}_\lambda$ are the low-energy excitations of the spin liquid, carrying spin-1 quantum numbers. In addition, the low-energy description contains a $U(1)$ gauge field, coupled to fermions $\tilde{f}_{i\lambda}$, and enforces the single-occupancy constraint.

Before proceeding further, let us reiterate the question of interest. We want to understand if the non-Fermi-liquid fixed point of a conventional overscreened Kondo model is changed by the presence of the gauge field in the bulk. The model outlined above provides us with a particular setup to study the influence of the non-Fermi-liquid bulk on the overscreened Kondo fixed point. However, in order to have control over calculations we need to resort to the large-N limit. The crucial requirement for the generalization procedure is to retain the presence of the overscreened Kondo fixed point. We choose a model with N species of *spin-1/2* fermions, $f_{i\alpha m}$, with $\alpha = \uparrow,\downarrow$ and $m = 1,\ldots,N$, as a large-N generalization. This is the simplest model which allows for controllable calculations.

The corresponding Lagrangian for our generalized model may be split into a fermionic part (including coupling to gauge field and impurity spin) and a gauge-field Lagrangian,

$$L = L_{\text{fermion}} + L_{\text{gauge}}. \tag{3}$$

The generalized fermion Lagrangian becomes

$$L_{\text{fermion}} = \int d\tau \sum_{\boldsymbol{k},m,\alpha} \Bigg[\bar{f}_{\boldsymbol{k}\alpha m} (\partial_\tau - \varepsilon_{\boldsymbol{k}}) f_{\boldsymbol{k}\alpha m} - \frac{e}{\sqrt{N}} \sum_{\boldsymbol{q}} f^\dagger_{\boldsymbol{k}+\frac{\boldsymbol{q}}{2}\alpha m} \boldsymbol{v}(\boldsymbol{k}) \cdot \boldsymbol{a}_{\boldsymbol{q}} f_{\boldsymbol{k}-\frac{\boldsymbol{q}}{2}\alpha m} - \frac{J_K}{N} \boldsymbol{S}(0) \cdot \boldsymbol{s} \Bigg], \tag{4}$$

where we use imaginary time. In accordance with the discussion above, fermion operators $f_{i\alpha m}$ now carry spin-1/2 quantum numbers ($\alpha = \uparrow,\downarrow$). We omit the time component of the gauge field from the coupling since it is screened[54] and do not write the diamagnetic term, including it in the gauge-field propagator. The fermion spin at $\boldsymbol{r} = 0$ is

$$\boldsymbol{S}(0) = \frac{1}{\mathcal{N}} \sum_{\boldsymbol{k},\boldsymbol{p},\alpha,\beta,m} f^\dagger_{\boldsymbol{k}\alpha m} \frac{\boldsymbol{\sigma}^{\alpha\beta}}{2} f_{\boldsymbol{p}\beta m}, \tag{5}$$

with $\boldsymbol{\sigma} = (\sigma^x,\sigma^y,\sigma^z)$ being the set of three Pauli matrices and $\mathcal{N}$ being the number of sites in the lattice. In what follows, Greek indices label spin projection, $\alpha,\beta,\ldots = \uparrow,\downarrow$, whereas

Latin indices $m,n,\ldots = 1,\ldots,N$ label channels. The coupling to the impurity J_K is assumed to be antiferromagnetic, $J_K > 0$.

The gauge-field Lagrangian is

$$L_{\text{gauge}} = \frac{1}{2}\int \frac{d\boldsymbol{q}\, d\omega}{(2\pi^3)} a_i^*(\boldsymbol{q},\omega) D_{ij}^{-1}(\boldsymbol{q},i\omega) a_j(\boldsymbol{q},\omega), \quad (6)$$

where the time component of the gauge field is excluded. The bare gauge-field propagator is zero since the gauge field is not dynamical, but rather represents fluctuations around the mean-field ansatz. However, nontrivial dynamics are generated if one accounts for coupling to fermions, leading to a nonzero $D_{ij}^{-1}(\boldsymbol{q},i\omega)$, which is discussed in Sec. I C.

B. Diagram technique

The impurity spin is conveniently represented via fermionic operators,

$$\boldsymbol{s} = \sum_{\alpha,\beta} c_\alpha^\dagger \frac{\boldsymbol{\sigma}^{\alpha\beta}}{2} c_\beta, \quad (7)$$

where $c_{\uparrow,\downarrow}^\dagger$ ($c_{\uparrow,\downarrow}$) are creation (annihilation) operators of spin-up or down pseudofermions.[2] In what follows we use the term "pseudofermions" to distinguish the operators c_α from the operators $f_{k\alpha m}$, which describe low-energy excitations in the spin liquid. A faithful representation of spin via fermion operators requires an additional constraint to exclude doubly occupied and empty states from the Hilbert space. However, in the case of a single spin-1/2 operator, $\boldsymbol{s}$, in Eq. (7), gives zero when acting on unphysical states in the Hilbert space. Therefore one can ignore the constraint in this case,[2] writing the impurity Lagrangian as

$$L_{\text{imp}} = \int d\tau\, \bar{c}_m(\partial_\tau - \mu_{\text{imp}}) c_m, \quad (8)$$

where μ_{imp} is the large positive energy corresponding to the chemical potential for impurity pseudofermions (see discussion in Ref. 2).

The rules for the diagram technique, following from Eqs. (4)–(8), are summarized in Fig. 1. Propagators for fermions and pseudofermions along with interaction vertices

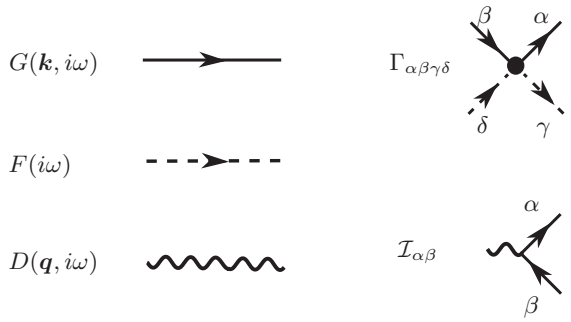

FIG. 1. Summary of rules for the diagram technique. Solid, dashed, and wavy lines represent a fermion, pseudofermion, and gauge-field propagator, respectively. Also, the interaction vertices of fermions with the gauge field, $\mathcal{I}_{\alpha\beta}$, and fermions with impurity pseudofermions, $\Gamma_{\alpha\beta\gamma\delta}$, are shown. All objects are diagonal in flavor indices, which are thus suppressed.

are given by

$$G_{\alpha\beta}^{mn}(\boldsymbol{k},i\omega) = \frac{\delta_{\alpha\beta}\delta_{mn}}{i\omega - \xi_{\boldsymbol{k}} - \Sigma(i\omega)}, \quad (9a)$$

$$F_{\alpha\beta}(i\omega) = \frac{\delta_{\alpha\beta}}{i\omega - \mu_{\text{imp}}}, \quad (9b)$$

$$\Gamma_{\alpha\beta\gamma\delta}^{mn} = -\frac{J_K}{4}\boldsymbol{\sigma}_{\alpha\beta}\cdot\boldsymbol{\sigma}_{\gamma\delta}\delta_{mn}, \quad (9c)$$

$$\mathcal{I}_{\alpha\beta}^{mn} = -\frac{e}{\sqrt{N}}\boldsymbol{v}_{\boldsymbol{k}}\delta_{\alpha\beta}\delta_{mn}, \quad (9d)$$

where $\xi_{\boldsymbol{k}} = \varepsilon_{\boldsymbol{k}} - \mu$ is the fermion energy relative to the Fermi surface. The self-energy, included in the fermion Green's function [Eq. (9a)], is discussed below. We note that the interaction between fermions and the impurity is local in real space. Therefore, in Fourier space, the momenta of two fermion operators in the impurity interaction vertex [Eq. (9c)] are unrelated. Fermion propagator and interaction vertices are diagonal in flavor indices. Thus the only contribution of flavor indices is an extra factor N for every loop of fermions, and they will be suppressed in the remainder of the paper.

C. Double expansion

We briefly review the double-expansion framework introduced in Ref. 57. First, we specify the dynamically generated propagator of the gauge field. To leading order, the propagator is given by the fermion bubble with current vertices along with the diamagnetic term shown in Fig. 2(a). In the Coulomb gauge, $\nabla\cdot\boldsymbol{a} = 0$, the propagator is transverse and can be written as[52,54,57]

$$D_{ij}^{-1}(\boldsymbol{q},i\omega) = \left(\delta_{ij} - \frac{q_i q_j}{q^2}\right) D_0^{-1}(\boldsymbol{q},\omega), \quad (10a)$$

$$D_0^{-1}(\boldsymbol{q},i\omega) = \gamma\frac{|\omega|}{q} + \chi_0 q^{z_b - 1}, \quad (10b)$$

with $z_b = 3$ and $\gamma = 2n/k_F$, $\chi_0 = 1/(24\pi m)$ for fermions with a quadratic dispersion. Note that the Landau damping term is nonzero only for $|\omega| < v_F q$. We assume z_b takes general value $z_b < 3$ and use it as a control parameter. This approach is consistent because terms q^{z_b-1} for $z_b < 3$ are nonlocal. Since z_b is not going to be renormalized within perturbation theory, it is a valid control parameter.

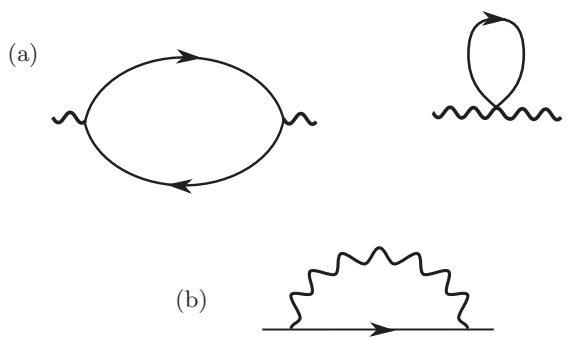

FIG. 2. (a) Self-energy of the gauge field due to interaction with fermions. The second diagram describes the diamagnetic contribution. (b) Self-energy of fermions due to interactions with the gauge field in the leading order in $1/N$.

The singular form of the gauge propagator [Eq. (10)] leads to a singular self-energy correction for fermions. In the leading order in $1/N$, the diagram in Fig. 2(b) gives us[54,56,57]

$$\Sigma(i\omega) = -i\lambda\,|\omega|^{2/z_b}\,\mathrm{sign}\,\omega, \tag{11a}$$

$$\lambda = \frac{e^2}{N}\frac{v_F}{\gamma}\frac{1}{4\pi\sin\frac{2\pi}{z_b}}\left(\frac{\gamma}{\chi_0}\right)^{2/z_b}. \tag{11b}$$

For $z_b > 2$, the self-energy is more important than the bare $i\omega$ term in the Green's function [Eq. (9a)] when $|\omega| < \omega_0$. The energy scale ω_0 is set by a combination of parameters γ, χ_0, and v_F [see Eq. (14)] and is of the order of Fermi energy, the only energy scale related to fermions.

When the self-energy, Eq. (11), is singular compared to the bare frequency dependence of the fermions' Green's function, a factor of $1/N$ in the fermion self-energy leads to an extra power of N in the *numerator* of the Green's function. This spoils naive power counting in the $1/N$ expansion,[56,58] requiring a summation of an infinite series of diagrams of a particular topology (genus) at any given order in $1/N$. However, if we assume a gauge-field dynamical exponent,[60] $z_b = 2 + \varepsilon$, and take the double scaling limit,[57]

$$\varepsilon \to 0, \quad N \to \infty, \quad \varepsilon N = \text{const}, \tag{12}$$

we obtain finite $\lambda \propto 1/(N\varepsilon)$ in Eq. (11b), rather than $\lambda \propto 1/N \to 0$. The absence of the factor $1/N$ in front of the self-energy restores naive power counting, where the gauge-field interaction vertex contributes $1/\sqrt{N}$ and each fermion loop gives a factor of N.

Finally, before proceeding further, we rewrite $\Sigma(i\omega)$ in a simplified form, valid in the double-scaling limit,

$$\Sigma(i\omega) = -i\frac{1}{N\varepsilon}\omega\left|\frac{\omega_0}{\omega}\right|^{\varepsilon/2}, \tag{13}$$

where the scale ω_0 is explicitly given by

$$\omega_0 = \frac{\chi_0}{\gamma}\left(\frac{e^2}{2\pi^2}\frac{v_F}{\chi_0}\right)^{2/\varepsilon}. \tag{14}$$

II. PERTURBATIVELY ACCESSIBLE FIXED POINT

The renormalization group (RG) approach in conjunction with $1/N$ expansion has been proven to be fruitful when applied to the conventional Kondo impurity problem. [2–4,11,61] The renormalization procedure is defined with respect to the fermion bandwidth D. Eliminating states far away from the Fermi surface, one studies the induced flow in the dimensionless coupling $g = \nu J_K$ (ν is the density of states per spin per channel assumed to be constant within the whole band). The corresponding β function is defined as

$$\beta(g) = \frac{d\ln g}{d\ln D} \tag{15}$$

and can be calculated perturbatively in g. This simplification is brought by the $1/N$ expansion and is justified in vicinity of a fixed point located at small $g^* \propto O(1/N)$.

When there is a gauge field coupled to fermions, the RG approach still can be applied. However, it requires some modifications. The usual $1/N$ expansion has to be replaced by the double expansion discussed above, but the RG flow is still defined with respect to bandwidth D. The coupling of the fermions to the gauge field e^2 is treated as a constant since a single impurity cannot change its flow under RG. Likewise, in the conventional Kondo problem, there exists a perturbatively accessible fixed point. After briefly reviewing the calculation for RG flow in the conventional Kondo problem, we calculate the β function in the presence of the gauge field and obtain physical properties in the vicinity of the fixed point.

A. β function in the conventional Kondo problem

While reviewing the RG procedure for the usual Kondo impurity problem, we mostly follow Refs. 2 and 3. Renormalization of the dimensionless coupling g in the leading order is given by diagrams shown in Fig. 3. Figures 3(a) and 3(b) represent corrections to the bare interaction vertex in the second and third orders of perturbation theory. These are the only diagrams up to the third order which are logarithmically divergent and thus renormalize the coupling. Note that Figs. 3(a) and 3(b) describe the contributions of the same order since the latter diagram, in addition to an extra power of $g \propto 1/N$, has a factor of N from the fermion loop. Figure 3(c) describes renormalization of the Z factor of pseudofermions and also contributes to the β function.

Calculation of the diagrams in Fig. 3 gives the β function:

$$\beta(g) = \frac{d\ln g}{d\ln D} = -g^2 + \frac{N}{2}g^3 + \cdots, \tag{16}$$

where the ellipsis denotes terms $C_1 N g^4 + C_2 N^2 g^5$ from higher-order diagrams. The coefficients $C_{1,2}$ are readily available in the literature [6,11,62] and are listed below in Eq. (20). As we shall see, these extra terms are subleading in the vicinity of a fixed point. One can easily solve for a stable non-Fermi-liquid fixed point of this β function:

$$g^* = \frac{2}{N} + \cdots, \tag{17}$$

$$\Delta_0 = \beta'(g^*) = \frac{2}{N} + \cdots, \tag{18}$$

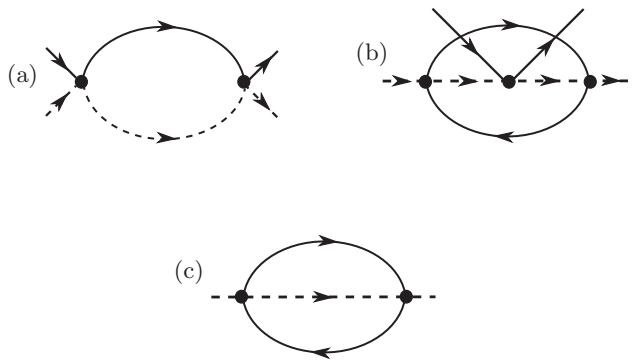

FIG. 3. Diagrams contributing to the β function in the leading order in $1/N$. (a) and (b) describe corrections to the vertex in the second and third orders of perturbation theory [the symmetric counterpart of (a) with the direction of one of the fermion lines changed is not shown]. (c) is the correction to the self-energy of pseudofermions, contributing to the β function via renormalization of the Z factor.

where Δ_0 is the slope of the β function at this fixed point. The ellipses here stand for terms $O(1/N^2)$. We see that g^* is indeed small in $1/N$, justifying the use of perturbation theory.

B. Correction to the β function due to the gauge field

As we shall see, within the double-expansion framework, the gauge field produces a small correction to the regular β function. Therefore it suffices to consider the effect of the gauge field to leading order.

There are two types of effects related to the gauge field. First, the gauge field destroys the well-defined quasiparticle, leading to non-Fermi-liquid behavior. This is manifested by the singular self-energy due to the gauge field in the fermion propagator [Eq. (13)]. Therefore one has to recalculate diagrams in Fig. 3 using the fermion propagator which contains the self-energy. A lengthy but straightforward calculation (see Appendix A for details) yields an answer identical to the case without gauge field, but with a modified divergent logarithm. Namely, the standard ln-divergent contributions are replaced by

$$\ln\frac{D}{\omega} \to \ln\frac{D}{\omega^{1-\kappa}\omega_0^{\kappa}}, \quad \kappa = \frac{1}{2N}\frac{1}{1+(N\varepsilon)^{-1}}, \tag{19}$$

where the energy scale $\omega_0 \propto D$ was defined in Eq. (14).

Another effect of the gauge field is the appearance of vertex corrections. All diagrams describing vertex corrections can be split into two classes, with representatives of each class depicted in Figs. 4(a) and 4(b), respectively. Diagrams belonging to the first class have at least one of the ends of the gauge-field propagator connected to the internal fermion line. In Appendix B we show that due to the transverse character of the gauge-field propagator and the locality of the interaction with the impurity, all diagrams of this type with a single gauge propagator exactly vanish.[30]

In the vertex correction diagrams attributed to the second class, the gauge-field propagator connects two external lines. One can think about these diagrams as describing a new interaction vertex [first diagram in Fig. 4(b)] and its renormalization (all other diagrams of this type). This new vertex contains an additional small factor $1/N$ compared to the original impurity interaction vertex. However, it is nonlocal since it depends strongly on the relation between outgoing and incoming fermion momenta, $\boldsymbol{k}$ and $\boldsymbol{p}$, respectively. The vertex is logarithmically divergent when the transferred momentum $|\boldsymbol{k}-\boldsymbol{p}|$ is close to $2k_F$ and is small otherwise.[52,54,57] The flow of this vertex to leading order in $1/N$ is identical to the flow of the standard vertex. Thus it does not influence the scaling in the vicinity of the fixed point. The effect of this vertex is to provide subleading corrections to different observables (due to the extra factor $1/N$). Therefore in what follows we do not consider this vertex.

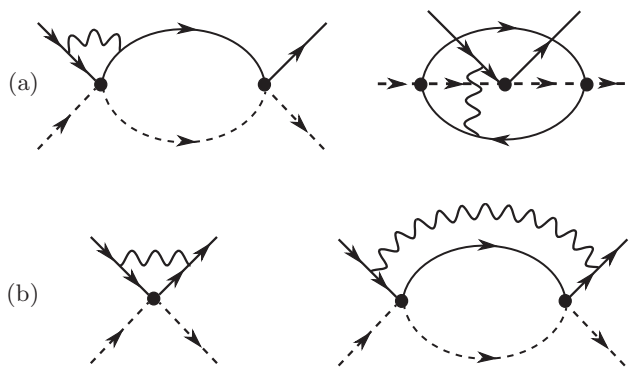

FIG. 4. Two types of vertex corrections in the leading order in $1/N$ due to the gauge field. (a) Example of vanishing diagrams with a single gauge propagator connected by at least one end to the internal line. (b) Nonvanishing corrections, representing a new nonlocal vertex (first diagram) and an example of a diagram leading to its renormalization (second diagram).

As we demonstrated, no new diagrams contribute to the β function up to order $1/N^3$. Calculation of diagrams in Fig. 3 with self-energy included in the fermionic propagator gives us

$$\beta(g) = (1-\kappa)\left(-g^2+\frac{N}{2}g^3\right) + \frac{N}{2}(1+\ln 2)g^4 - \frac{N^2}{4}g^5, \tag{20}$$

where terms in the second line come from higher-order diagrams and are $O(1/N^3)$ in the vicinity of the fixed point. The terms in the first line are universal with respect to the reparametrization of the coupling constant g.[19] These terms have to be included for consistency since $\kappa \propto 1/N$ but are identical to those in the β function without the gauge field, Eq. (16) [accounting for gauge field in these terms will produce corrections $O(1/N^4)$].

The obtained β function, Eq. (20), differs from the β function without the gauge field, Eq. (16), by terms $O(1/N^3)$. This correction does not shift the fixed point g^* even at order $1/N^2$ compared to the fixed point, Eq. (17).[63] However, it modifies the slope of $\beta(g)$ at the fixed point,

$$\Delta_1 = \frac{2}{N}(1-\kappa) + \cdots = (1-\kappa)\Delta_0, \tag{21}$$

compared to the slope for the case of the conventional Kondo problem Δ_0 [Eq. (18)]. Below, the slope of the β function Δ_1 will be used to determine the flow of the coupling in the vicinity of the fixed point as well as the singular behavior of different measurable quantities.[11] Therefore the difference between Δ_0 and Δ_1 modifies the behavior of different observables compared to the conventional Kondo problem.

C. Observables

In order to understand how the non-Fermi-liquid fixed point manifests itself in observables, we first find the dependence of the running coupling constant $g_R(\omega)$ on ω. It can be determined from the flow equation $dg_R(\omega)/d\ln\omega = -\beta(g_R)$ by employing the results for the β function and its slope at the fixed point. Denoting the bare value of coupling at $\omega = D$ as $g_R(D) = g$, we have[11]

$$g_R(\omega) = g^* - \zeta\left(\frac{\omega}{T_K}\right)^{\Delta}, \tag{22}$$

where Δ is the slope of the β function, which depends on the presence of the coupling to the gauge field. The position of the fixed point g^*, Eq. (17), is not influenced by the gauge field. The Kondo temperature is $T_K = D(T_K^{(0)}/D)^{\Delta_0/\Delta}$, where $T_K^{(0)} = Dg^{N/2}\exp(-1/g)$ is the Kondo scale for the case

without a gauge field, and $\zeta = (g^*)^2/e$. We assumed here that $\omega < T_K$ and that the initial value of coupling g is small.

The power-law behavior of the running coupling leads to a similar behavior in different physical quantities. Corrections to different measurable properties within perturbation theory can be expressed as a series in coupling g. Applying the renormalization group to this series results in singular behavior as a function of frequency or temperature with the exponent proportional to Δ. For the case when there is no gauge field present, this procedure has been implemented in Ref. 11. Generalization of this procedure to the case with the gauge field is straightforward.

The main effect of the gauge field is always related to the different values of the slope of the β function Δ. Without a gauge field $\Delta = \Delta_0$ is given by Eq. (18). When there is a gauge field, we have $\Delta = \Delta_1$, specified in Eq. (21). While for thermodynamical quantities this is the only effect, transport properties and other quantities acquire small corrections to prefactors which are not given here.

Calculating the contribution of impurity to the imaginary part of the self-energy of the fermions gives the scattering rate due to the impurity. As a function of frequency, it acquires a cusp at $\omega = 0$,

$$\nu\tau_{\text{imp}}^{-1}(\omega) = \frac{3\pi n_{\text{imp}}}{2N^2}\left[1 - N\zeta\left(\frac{\omega}{T_K}\right)^{\Delta}\right], \tag{23}$$

which has to be contrasted with a Lorentzian shape of $\nu\tau_{\text{imp}}^{-1}(\omega)$ for a Fermi-liquid fixed point. The correction to the resistivity due to the Kondo interaction has a similar form; however, it is of little interest due to the neutral character of fermionic excitations in a spin liquid. The correction to the heat conductivity is potentially more interesting. Using Eq. (23) and assuming that impurity scattering time τ_{imp} is much longer than the relaxation time without impurity τ_0, we find the correction to the inverse two-dimensional thermal conductivity,

$$\delta\left[\kappa_{\text{th}}^{-1}\right] = \frac{9}{N^2}\frac{\hbar}{k_B^2 T}\frac{n_{\text{imp}}}{n}\left[1 - N\zeta\left(\frac{T}{T_K}\right)^{\Delta}\right], \tag{24}$$

where we restored $\hbar$ and k_B is the Boltzmann constant.

Also one can calculate corrections to different thermodynamic properties. A rigorous calculation of the self-energy allows us to find the impurity specific heat with a critical exponent $\alpha = 2\Delta$:

$$C_{\text{imp}} = \frac{3\pi^2}{2}\zeta^2\Delta\left(\frac{T}{T_K}\right)^{2\Delta}. \tag{25}$$

The magnetic properties, such as the impurity susceptibility as temperature $T \to 0$ and the dependence of magnetization on the field $h = \mu_B H$ at $T = 0$, are given by

$$\chi_{\text{imp}} = \left(\frac{N\zeta}{2}\right)^2\frac{1}{T}\left(\frac{T}{T_K}\right)^{2\Delta}, \tag{26}$$

$$M = \frac{N\zeta}{2}\left(\frac{h}{T_K}\right)^{\Delta}. \tag{27}$$

Likewise, it is possible to find an expression for fermion-fermion, fermion-impurity, and impurity-impurity susceptibilities.[11] Last, we list results for $\chi''_{\text{imp}}(\omega,T)/\omega$, which is a contribution to the NMR relaxation rate due to the impurity. Its behavior is again specified by Δ, and for $\omega \ll T$

$$\frac{\chi''_{\text{imp}}(\omega,T)}{\omega} \propto T^{2\Delta-2}. \tag{28}$$

III. DISCUSSION

We have investigated the effect of the gauge field strongly coupled to fermions at a non-Fermi-liquid overscreened Kondo fixed point. Using the double-expansion framework, we demonstrated that the gauge field does not alter the position of the perturbatively accessible non-Fermi-liquid fixed point but leads to corrections to exponents characterizing the behavior of different physical properties in the vicinity of the fixed point. In particular, it "softens" the nonanalytic behavior of specific heat, magnetization, and spin susceptibility compared to those for a Kondo problem without the gauge field. The physical origin of this effect is the "smearing" of the sharp quasiparticles by the gauge field.

Let us discuss the extrapolation to the physical case. In order to have a control over calculations, we worked in the double-expansion limit, Eq. (12), with N species of spin-1/2 fermions. We note that if the coupling to the gauge field is absent, the considered model for $N = 4$ corresponds to the one channel of spin-1 itinerant moments coupled to impurity.[9,12] The same equivalence was found to hold in our perturbative calculations of the β function for the case when there is a coupling to the gauge field.

Thus we expect that the physical case corresponds to $N = 4, \varepsilon = 1$. Assuming that our results can be extrapolated to these values of N and ε, we can argue that the non-Fermi-liquid Kondo fixed point is not destroyed by the presence of a gauge field. However, we expect singularities in different physical properties related to the non-Fermi-liquid fixed point to be weakened compared to their values without a gauge field. In such a case, the realization of overscreened Kondo physics in an $S = 1$ spin liquid may be used not only to observe neutral fermionic excitations but as evidence for the presence of a gauge field. Indeed, non-Fermi-liquid behavior may be used as an indication of fermionic excitations present in the system. At the same time, the difference of observed scalings from those for the case without a gauge field [6,12] may be used as a litmus test for the presence of a gauge field coupled to fermions. From an experimental point of view, specific heat (proportional to impurity concentration), spin susceptibility, and the NRM relaxation rate are the most promising probes.

It is instructive to compare the role of the gauge field in our case to the case of the Kondo model in the regime of perfect screening in Ref. 30. In the latter case, the system flows to the infinite-coupling fixed point, and the results of Ref. 30 show no changes in impurity specific heat and spin susceptibility due to the presence of the gauge field.

Finally, we discuss possible experimental realizations of our proposal. In recent experiments[32,33] materials that could possibly realize the spin liquid with fermionic excitations[37,39,41] have been found. One can speculate on the possible stabilization of the $U(1)$ spin-liquid phase in the same or similar types of materials. The presence of spin-1/2 impurities in such a phase would realize the scenario considered in our

work. Another way to implement the discussed physics is to go to lower dimensions. A gapless phase for spin-1 chain with bilinear and biquadratic interaction has been established for a certain range of couplings.[64–67] A spin-1/2 impurity in such a chain is expected to realize overscreened Kondo physics. A detailed consideration of this problem will be presented elsewhere.

ACKNOWLEDGMENTS

M.S. acknowledges discussions with David Mross and John McGreevy. This work was supported by NSF Grant No. DMR 1005434 (T.S.) and NSF Grant No. DMR 1104498 (P.A.L.).

APPENDIX A: CALCULATION OF DIAGRAMS FOR THE β FUNCTION

In this Appendix we present the calculation of the diagrams in Fig. 3 with the fermion propagator, Eq. (9a), containing self-energy due to the gauge field. A detailed calculation of these diagrams without a gauge field can be found, for example, in Refs. 2 and 3.

First, we consider the diagram in Fig. 3(a), which describes the second-order correction to the dimensionless coupling $g = \nu J_K$. We will be interested only in the logarithmically divergent part of the diagram. Using the zero-temperature Matsubara diagram technique and implying summation over repeated indices, we can write, for the correction to the impurity interaction vertex,

$$\Gamma^{(a1)}_{\alpha\beta\gamma\delta} = -\left(\frac{J_K}{4}\right)^2 (\boldsymbol{\sigma}_{\alpha\rho}\cdot\boldsymbol{\sigma}_{\gamma\lambda})(\boldsymbol{\sigma}_{\rho\beta}\cdot\boldsymbol{\sigma}_{\lambda\delta}) \times \int \frac{d\boldsymbol{k}\, d\omega_1}{(2\pi)^3} F(-i\omega_1) G(\boldsymbol{k}, i\omega + i\omega_1). \quad \text{(A1)}$$

The symmetric counterpart of the diagram in Fig. 3(a) with a flipped direction of the propagation of the pseudofermions (not shown) gives us

$$\Gamma^{(a2)}_{\alpha\beta\gamma\delta} = -\left(\frac{J_K}{4}\right)^2 (\boldsymbol{\sigma}_{\alpha\rho}\cdot\boldsymbol{\sigma}_{\lambda\delta})(\boldsymbol{\sigma}_{\rho\beta}\cdot\boldsymbol{\sigma}_{\gamma\lambda}) \times \int \frac{d\boldsymbol{k}\, d\omega_1}{(2\pi)^3} F(i\omega_1) G(\boldsymbol{k}, i\omega + i\omega_1). \quad \text{(A2)}$$

After integrating over ω_1 and changing the integration variable from $\boldsymbol{k}$ to $\xi = \varepsilon_{\boldsymbol{k}} - \mu$, we have similar expressions for both diagrams:

$$\Gamma^{(a1,2)}_{\alpha\beta\gamma\delta} = \left(\frac{J_K}{4}\right)^2 (\mp 2\boldsymbol{\sigma}_{\alpha\beta}\cdot\boldsymbol{\sigma}_{\gamma\delta} + 3\delta_{\alpha\beta}\delta_{\gamma\delta}) \times \nu \int d\xi \frac{\theta(\pm\xi)}{i\omega\left(1 + \frac{1}{N\varepsilon}\left|\frac{\omega_0}{\omega}\right|^{\varepsilon/2}\right) - \xi}. \quad \text{(A3)}$$

We perform the integration over ξ, retaining only the logarithmic part. Collecting results for both diagrams and going to the real-frequency domain, we get

$$\Gamma^{(a)}_{\alpha\beta\gamma\delta} = 4\nu\left(\frac{J_K}{4}\right)^2 (\boldsymbol{\sigma}_{\alpha\beta}\cdot\boldsymbol{\sigma}_{\gamma\delta}) \times \ln\frac{D}{|\omega|\left(1 + \frac{1}{N\varepsilon}\left|\frac{\omega_0}{\omega}\right|^{\varepsilon/2}\right)}. \quad \text{(A4)}$$

We expand the logarithm in ε to the leading order and collect both terms into a single logarithm again:

$$\ln\frac{D}{|\omega|\left(1 + \frac{1}{N\varepsilon}\left|\frac{\omega_0}{\omega}\right|^{\varepsilon/2}\right)} = \ln\frac{D}{|\omega|} - \kappa\ln\frac{\omega_0}{|\omega|} = \ln\frac{D}{|\omega|^{1-\kappa}\omega_0^{\kappa}}, \quad \text{(A5)}$$

where κ is small, $\kappa \propto O(1/N)$,

$$\kappa = \frac{1}{2N}\frac{1}{1 + \frac{1}{N\varepsilon}}. \quad \text{(A6)}$$

Finally, we have

$$\Gamma^{(a)}_{\alpha\beta\gamma\delta} = -g\ln\frac{D}{|\omega|^{1-\kappa}\omega_0^{\kappa}}\Gamma_{\alpha\beta\gamma\delta}, \quad \text{(A7)}$$

where the bare vertex $\Gamma_{\alpha\beta\gamma\delta}$ is defined in Eq. (9c), and we retained only logarithmically divergent terms. Alternatively, we could expand the Green's function in $1/N$ before performing integration over frequency and momenta [Eqs. (A1) and (A2)], reproducing the same result.

Calculations of the vertex and Z-factor renormalization, described by Figs. 3(b) and 3(c), respectively, are very similar. Indeed, in order to get the impurity pseudofermion Z factor, Z_{imp}, we have to differentiate self-energy over ω, which may be thought of as an introduction of an additional vertex with zero incoming frequency. Therefore below we present only the details of the calculation for the derivative of self-energy and list the result for the vertex renormalization.

The correction to the impurity self-energy described by Fig. 3(c) is written as

$$\Sigma^{\text{imp}}(i\omega) = -6N\left(\frac{J_K}{4}\right)^2 \int \frac{d\boldsymbol{k}_1\, d\omega_1}{(2\pi)^3}\frac{d\boldsymbol{k}_2\, d\Omega_2}{(2\pi)^3} \times G(\boldsymbol{k}_1, i\omega_1) G(\boldsymbol{k}_2, i\omega_1 + i\Omega_2) F(i\omega + i\Omega_2), \quad \text{(A8)}$$

where we omitted the spin indices of external pseudofermions and the associated δ function. Renormalization of Z_{imp} is given by the derivative of the self-energy,

$$Z^{-1}_{\text{imp}} = 1 - \frac{\partial\Sigma_{\text{imp}}(i\omega)}{\partial(i\omega)}, \quad \text{(A9)}$$

so that, to first order in the self-energy,

$$\delta Z_{\text{imp}} = \frac{\partial\Sigma^{\text{imp}}(i\omega)}{\partial(i\omega)}. \quad \text{(A10)}$$

Integrating over Ω_2 in Eq. (A8), we have

$$\delta Z_{\text{imp}} = 6N\left(\frac{J_K}{4}\right)^2 \frac{\partial}{\partial(i\omega)} \int \frac{d\boldsymbol{k}_1\, d\boldsymbol{k}_2}{(2\pi)^4} \mathcal{I}_{\boldsymbol{k}_1,\boldsymbol{k}_2,i\omega}, \quad \text{(A11)}$$

$$\mathcal{I}_{\boldsymbol{k}_1,\boldsymbol{k}_2,i\omega} = \int \frac{d\omega_1}{2\pi} G(\boldsymbol{k}_1, i\omega_1) G(\boldsymbol{k}_2, i\omega_1 - i\omega)\theta(-\xi_{\boldsymbol{k}_2}). \quad \text{(A12)}$$

To simplify further calculations, we expand in ε and $1/N$. The self-energy, Eq. (13), expanded to the leading order in ε becomes

$$\Sigma(i\omega) = -i\omega\left(\frac{1}{N\varepsilon} + \frac{1}{2N}\ln\left|\frac{\omega_0}{\omega}\right|\right). \tag{A13}$$

Inserting this into the fermion Green's function, Eq. (9a), and expanding in $1/N$, we get

$$G(\boldsymbol{k}_1,i\omega_1) = \tilde{G}(\boldsymbol{k}_1,i\omega_1) - \frac{1}{2N}i\omega_1\ln\left|\frac{\omega_0}{\omega_1}\right|[\tilde{G}(\boldsymbol{k}_1,i\omega_1)]^2, \tag{A14}$$

where $\tilde{G}(\boldsymbol{k}_1,i\omega_1)$ is defined as

$$\tilde{G}(\boldsymbol{k}_1,i\omega_1) = \frac{1}{i\omega_1\left(1+\frac{1}{N\varepsilon}\right) - \xi_{\boldsymbol{k}_1}}. \tag{A15}$$

Finally, expansion of the product of the Green's function in $\mathcal{I}_{\boldsymbol{k}_1,\boldsymbol{k}_2,i\omega}$, Eq. (A12), gives us

$$\mathcal{I}_{\boldsymbol{k}_1,\boldsymbol{k}_2,i\omega} = \int\frac{d\omega_1}{2\pi}\theta(-\xi_{\boldsymbol{k}_2})\tilde{G}(\boldsymbol{k}_1,i\omega_1)\tilde{G}(\boldsymbol{k}_2,i\omega_1 - i\omega) \times\left[1 - \frac{1}{2N}i\omega_1\ln\left|\frac{\omega_0}{\omega_1}\right|\tilde{G}(\boldsymbol{k}_1,i\omega_1) - \frac{1}{2N}i(\omega_1-\omega)\ln\left|\frac{\omega_0}{\omega_1-\omega}\right|\tilde{G}(\boldsymbol{k}_2,i\omega_1 - i\omega)\right]. \tag{A16}$$

After integration over ω_1, the zeroth-order term in (A16) yields

$$\mathcal{I}^{(0)}_{\boldsymbol{k}_1,\boldsymbol{k}_2,i\omega} = -\frac{\theta(\xi_{\boldsymbol{k}_1})\theta(-\xi_{\boldsymbol{k}_2})}{\left(1+\frac{1}{N\varepsilon}\right)\left[\xi_{\boldsymbol{k}_1} + |\xi_{\boldsymbol{k}_2}| - i\left(1+\frac{1}{N\varepsilon}\right)\omega\right]}. \tag{A17}$$

This is inserted into Eq. (A11). After integration over momenta the extra factors $(1+\frac{1}{N\varepsilon})$ drop out, and we reproduce the answer for the case without a gauge field, $\delta Z^{(0)}_{\rm imp} = -3Ng^2/8\ln(D/|\omega|)$.

Frequency integration for terms proportional to $1/N$ in Eq. (A16) results in a cumbersome expression. However, after integrations over $\xi_{\boldsymbol{k}_1}$ and $\xi_{\boldsymbol{k}_2}$ and extracting the ln-divergent part we obtain $\delta Z^{(1)}_{\rm imp} = 3\kappa Ng^2/8\ln(\omega_0/|\omega|)$, where κ is defined in Eq. (A6). Combining $\delta Z^{(0)}_{\rm imp}$ and $\delta Z^{(1)}_{\rm imp}$, we have, for the impurity pseudofermion Z factor,

$$Z_{\rm imp} = 1 + \delta Z_{\rm imp} = 1 - \frac{3}{8}Ng^2\ln\frac{D}{|\omega|^{1-\kappa}\omega_0^{\kappa}}. \tag{A18}$$

The correction to the impurity interaction vertex [Fig. 3(b)] is calculated in a similar way. The resulting contribution to the interaction vertex is

$$\Gamma^{(b)}_{\alpha\beta\gamma\delta} = \frac{N}{8}g^2\ln\frac{D}{|\omega|^{1-\kappa}\omega_0^{\kappa}}\Gamma_{\alpha\beta\gamma\delta}. \tag{A19}$$

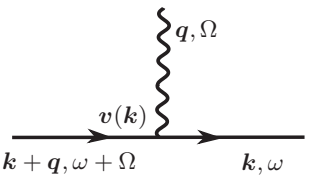

FIG. 5. Part of the diagram with vertex corrections that makes the diagram vanish.

Finally, the renormalized coupling is

$$g_R = \frac{g+\delta g}{Z_{\rm imp}}, \tag{A20}$$

where $Z_{\rm imp}$ is given by Eq. (A18) and δg can be read from Eqs. (A7) and (A19):

$$\frac{\delta g}{g} = \left(-g + \frac{N}{8}g^2\right)\ln\frac{D}{|\omega|^{1-\kappa}\omega_0^{\kappa}}. \tag{A21}$$

Using that $\omega_0 \propto D$, we obtain the β function:

$$\beta(g) = \frac{d\ln g}{d\ln D} = (1-\kappa)\left(-g^2 + \frac{N}{2}g^3\right) + \cdots, \tag{A22}$$

where the ellipsis denotes the subleading terms $O(1/N^3)$ obtained in Ref. 11 and listed in the main text. Note that Eq. (A22) is exact to the order $1/N^3$: corrections to subleading terms from the gauge field are of order $O(1/N^4)$ and thus can be ignored.

APPENDIX B: VERTEX CORRECTIONS

In this Appendix we demonstrate that a subset of vertex corrections where the gauge-field propagator is connected to the internal fermion Green's function vanishes. Two examples of such diagrams are shown in Fig. 4(a). It suffices to consider a part present in all diagrams, consisting of two Green's functions and a single gauge-field vertex (Fig. 5). Using notations adopted in Fig. 5, we can write for the integral over momentum $\boldsymbol{k}$

$$\int dk_x\,dk_y\,v_y(\boldsymbol{k})G(\boldsymbol{k},i\omega)G(\boldsymbol{k}+q\boldsymbol{e}_x,i\omega+i\Omega), \tag{B1}$$

where we assumed that $\boldsymbol{q}$ has only the x component, $\boldsymbol{q}\|\boldsymbol{e}_x$, and used the fact that the gauge field is transverse. Note that integration over $\boldsymbol{k}$ does not involve any other functions due to the fact that interaction with impurity is local. It is integration over k_y in Eq. (B1) that makes the expression zero. Indeed, prefactor $v_y(\boldsymbol{k})$ is odd under the inversion of k_y, whereas neither Green's function changes under $k_y \to -k_y$. Since this part is present in all diagrams in Fig. 4(b), all these diagrams vanish.

[1] J. Kondo, Prog. Theor. Phys. **40**, 683 (1968).
[2] A. A. Abrikosov, Physics **2**, 5 (1965).
[3] A. A. Abrikosov and A. A. Migdal, J. Low Temp. Phys. **3**, 519 (1970).
[4] P. Nozières and A. Blandin, J. Phys. (Paris) **41**, 19 (1980).
[5] N. Read and D. M. Newns, J. Phys. C **16**, 3273 (1983).
[6] I. Affleck, Nucl. Phys. B **336**, 517 (1990); I. Affleck and A. W. Ludwig, *ibid.* **360**, 641 (1991); **352**, 849 (1991).

[7] O. Parcollet and A. Georges, Phys. Rev. Lett. **79**, 4665 (1997).
[8] O. Parcollet, A. Georges, G. Kotliar, and A. Sengupta, Phys. Rev. B **58**, 3794 (1998).
[9] A. M. Sengupta and Y. B. Kim, Phys. Rev. B **54**, 14918 (1996).
[10] M. Fabrizio and G. Zaránd, Phys. Rev. B **54**, 10008 (1996).
[11] J. Gan, N. Andrei, and P. Coleman, Phys. Rev. Lett. **70**, 686 (1993); J. Gan, J. Phys. Condens. Matter **6**, 4547 (1994).
[12] M. Fabrizio and A. O. Gogolin, Phys. Rev. B **50**, 17732 (1994).
[13] R. M. Potok, I. G. Rau, H. Shtrikman, Y. Oreg, and D. Goldhaber-Gordon, Nature (London) **446**, 167 (2007).
[14] A. C. Hewson, *The Kondo Problem to Heavy Fermions* (Cambridge University Press, Cambridge, 1993).
[15] D. L. Cox and A. Zawadowski, Adv. Phys. **47**, 599 (1998).
[16] P. Schlottmann and P. D. Sacramento, Adv. Phys. **42**, 641 (1993).
[17] A. Tsvelick and P. Wiegmann, Adv. Phys. **32**, 453 (1983); Z. Phys. B **54**, 201 (1984); J. Stat. Phys. **38**, 125 (1985).
[18] A. Tsvelick, J. Phys. C **18**, 159 (1985).
[19] N. Andrei, K. Furuya, and J. H. Lowenstein, Rev. Mod. Phys. **55**, 331 (1983).
[20] B. Béri and N. R. Cooper, Phys. Rev. Lett. **109**, 156803 (2012).
[21] M. Vojta, Philos. Mag. **86**, 1807 (2006).
[22] D. Withoff and E. Fradkin, Phys. Rev. Lett. **64**, 1835 (1990).
[23] C. R. Cassanello and E. Fradkin, Phys. Rev. B **53**, 15079 (1996); M. Vojta and L. Fritz, *ibid.* **70**, 094502 (2004); L. Fritz and M. Vojta, *ibid.* **70**, 214427 (2004); L. Fritz, S. Florens, and M. Vojta, *ibid.* **74**, 144410 (2006).
[24] G. Khaliullin, R. Kilian, S. Krivenko, and P. Fulde, Phys. Rev. B **56**, 11882 (1997); N. Nagaosa and T.-K. Ng, *ibid.* **51**, 15588 (1995); N. Nagaosa and P. A. Lee, Phys. Rev. Lett. **79**, 3755 (1997); C. Pépin and P. A. Lee, *ibid.* **81**, 2779 (1998); Z. Wang and P. A. Lee, *ibid.* **89**, 217002 (2002).
[25] S. Sachdev, C. Buragohain, and M. Vojta, Science **286**, 2479 (1999); S. Sachdev and M. Vojta, Phys. Rev. B **68**, 064419 (2003); K. H. Höglund and A. W. Sandvik, Phys. Rev. Lett. **99**, 027205 (2007); K. H. Höglund, A. W. Sandvik, and S. Sachdev, *ibid.* **98**, 087203 (2007); M. A. Metlitski and S. Sachdev, Phys. Rev. B **77**, 054411 (2008).
[26] S. Florens, L. Fritz, and M. Vojta, Phys. Rev. Lett. **96**, 036601 (2006); Phys. Rev. B **75**, 224420 (2007).
[27] A. Kolezhuk, S. Sachdev, R. R. Biswas, and P. Chen, Phys. Rev. B **74**, 165114 (2006).
[28] K.-S. Kim and M. D. Kim, J. Phys. Condens. Matter **20**, 125206 (2008).
[29] K. Dhochak, R. Shankar, and V. Tripathi, Phys. Rev. Lett. **105**, 117201 (2010).
[30] P. Ribeiro and P. A. Lee, Phys. Rev. B **83**, 235119 (2011).
[31] P. W. Anderson, Mater. Res. Bull. **8**, 153 (1973); Science **235**, 1196 (1987).
[32] S. Nakatsuji, Y. Nambu, H. Tonomura, O. Sakai, S. Jonas, C. Broholm, H. Tsunetsugu, Y. Qiu, and Y. Maeno, Science **309**, 1697 (2005).
[33] J. G. Cheng, G. Li, L. Balicas, J. S. Zhou, J. B. Goodenough, C. Xu, and H. D. Zhou, Phys. Rev. Lett. **107**, 197204 (2011).
[34] S. Bhattacharjee, V. B. Shenoy, and T. Senthil, Phys. Rev. B **74**, 092406 (2006).
[35] E. M. Stoudenmire, S. Trebst, and L. Balents, Phys. Rev. B **79**, 214436 (2009).
[36] H. Tsunetsugu and M. Arikawa, J. Phys. Soc. Jpn. **75**, 083701 (2006).
[37] Z.-X. Liu, Y. Zhou, and T.-K. Ng, Phys. Rev. B **81**, 224417 (2010); **82**, 144422 (2010).
[38] T. Grover and T. Senthil, Phys. Rev. Lett. **107**, 077203 (2011).
[39] M. Serbyn, T. Senthil, and P. A. Lee, Phys. Rev. B **84**, 180403 (2011).
[40] C. Xu, F. Wang, Y. Qi, L. Balents, and M. P. A. Fisher, Phys. Rev. Lett. **108**, 087204 (2012).
[41] S. Bieri, M. Serbyn, T. Senthil, and P. A. Lee, Phys. Rev. B **86**, 224409 (2012).
[42] O. I. Motrunich, Phys. Rev. B **73**, 155115 (2006).
[43] M. R. Norman and T. Micklitz, Phys. Rev. Lett. **102**, 067204 (2009).
[44] W.-H. Ko, Z.-X. Liu, T.-K. Ng, and P. A. Lee, Phys. Rev. B **81**, 024414 (2010).
[45] W.-H. Ko and P. A. Lee, Phys. Rev. B **84**, 125102 (2011).
[46] D. F. Mross and T. Senthil, Phys. Rev. B **84**, 041102 (2011).
[47] Y. Zhou and P. A. Lee, Phys. Rev. Lett. **106**, 056402 (2011).
[48] P. Coleman and C. Pépin, Phys. Rev. B **68**, 220405 (2003).
[49] P. Mehta, N. Andrei, P. Coleman, L. Borda, and G. Zarand, Phys. Rev. B **72**, 014430 (2005).
[50] D. C. Ralph and R. A. Buhrman, Phys. Rev. Lett. **69**, 2118 (1992). D. C. Ralph, A. W. W. Ludwig, J. von Delft, and R. A. Buhrman, *ibid.* **72**, 1064 (1994).
[51] P. A. Lee and N. Nagaosa, Phys. Rev. B **46**, 5621 (1992).
[52] B. L. Altshuler, L. B. Ioffe, and A. J. Millis, Phys. Rev. B **50**, 14048 (1994).
[53] B. L. Altshuler, L. B. Ioffe, and A. J. Millis, Phys. Rev. B **52**, 5563 (1995).
[54] Y. B. Kim, A. Furusaki, X.-G. Wen, and P. A. Lee, Phys. Rev. B **50**, 17917 (1994).
[55] O. I. Motrunich, Phys. Rev. B **72**, 045105 (2005).
[56] S.-S. Lee, Phys. Rev. B **80**, 165102 (2009).
[57] D. F. Mross, J. McGreevy, H. Liu, and T. Senthil, Phys. Rev. B **82**, 045121 (2010).
[58] M. A. Metlitski and S. Sachdev, Phys. Rev. B **82**, 075127 (2010).
[59] X. Wen, *Quantum Field Theory of Many-Body Systems: From the Origin of Sound to an Origin of Light and Electrons*, Oxford Graduate Texts (Oxford University Press, Oxford, 2004) .
[60] In notations adopted in Ref. 54, $\eta = z_b - 1 = 1 + \varepsilon$.
[61] P. Nozieres, J. Low Temp. Phys. **17**, 112 (1974).
[62] N. Andrei and C. Destri, Phys. Rev. Lett. **52**, 364 (1984).
[63] The fact that g^* does not change up to $O(1/N^2)$ becomes clear if we multiply the second line of Eq. (20) by $(1 - \kappa)$ as well. Such operation is allowed as it leaves intact all terms up to $O(1/N^3)$.
[64] G. Fáth and J. Sólyom, Phys. Rev. B **44**, 11836 (1991); **47**, 872 (1993).
[65] C. Itoi and M.-H. Kato, Phys. Rev. B **55**, 8295 (1997).
[66] I. Affleck, M. Oshikawa, and H. Saleur, J. Phys. A **34**, 1073 (2001).
[67] A. Läuchli, G. Schmid, and S. Trebst, Phys. Rev. B **74**, 144426 (2006).